

# Search for GUT monopoles at Super-Kamiokande

Koh Ueno\* for the Super-Kamiokande collaboration

\*Kamioka Observatory, ICRR, University of Tokyo, Higashi-Mozumi, Kamioka, Hida, Gifu 506-1205, Japan

**Abstract.** GUT monopoles captured by the Sun's gravitation are expected to catalyze proton decays via the Callan-Rubakov process. In this scenario, protons, which initially decay into pions, will ultimately produce  $\nu_e$ ,  $\nu_\mu$  and  $\bar{\nu}_\mu$ . After going through neutrino oscillation, all neutrino species appear when they arrive at the Earth, and can be detected by a 50,000 ton water Cherenkov detector, Super-Kamiokande (SK). A search for neutrinos produced through such a process has been carried out with SK and is expected to give the cross section and velocity dependent limit on the monopole flux,  $F < 1 \times 10^{-23} \text{ cm}^{-2} \text{ s}^{-1} \text{ sr}^{-1}$  for  $\beta = 10^{-3}$  and  $\sigma = 1 \text{ mb}$  at 90% C.L. This is one order of magnitude more stringent a limit than the previous result, which was obtained by the Kamiokande experiment.

**Keywords:** GUT monopole, neutrino, water Cherenkov detector

## I. INTRODUCTION

Grand Unified Theories (GUT) predict superheavy monopoles (GUT monopoles) produced in the very early universe. GUT monopoles are predicted to have appeared as topological defects at the phase transition of vacuum, where GUT gauge group spontaneously broke to leave the U(1) of electromagnetism. If we take as an example the temperature of the phase transition at which the monopoles were formed equal to  $10^{15} \text{ GeV}$  and assume the average production rate of about one monopole per horizon at that time [1], the density of the monopoles today exceeds critical density of the universe by more than 14 orders of magnitude. Even though the inflationary universe scenario [2], [3] overcomes this problem, the monopole flux in the universe depends on some parameters such as monopole mass or the reheating temperature, and therefore the uncertainty remains. In fact, due to the wide variety of elementary particle models, several models coexist with the Parker limit ( $\sim 10^{-15} \text{ cm}^{-2} \text{ s}^{-1} \text{ sr}^{-1}$ ) [4], [5], [6], and a flux in that range can be relatively easily detected by underground experiments. Arafune et al. [7] pointed out copious low energy neutrinos might be emitted when monopoles accumulating inside the Sun catalyze proton decay;

$$p \rightarrow (\rho^0, \omega, \eta, K^+, \dots) + e^+ (\text{or } \mu^+) \quad (1)$$

along their paths with cross sections typical of strong interactions via so called Callan-Rubakov process [8], [9]. But, contrary to spontaneous proton decay, direct neutrino production process, such as  $p \rightarrow \bar{\nu} + \pi^+$ , is forbidden [8]. When decay mesons produced by the

process above subsequently decay into positive pions,  $(\rho^0, \omega, \eta, K^+, \dots) \rightarrow \pi^+, \nu_e, \nu_\mu$  and  $\bar{\nu}_\mu$  are produced as described below,

$$\pi^+ \rightarrow \mu^+ + \nu_\mu \quad (2)$$

$$\mu^+ \rightarrow e^+ + \nu_e + \bar{\nu}_\mu \quad (3)$$

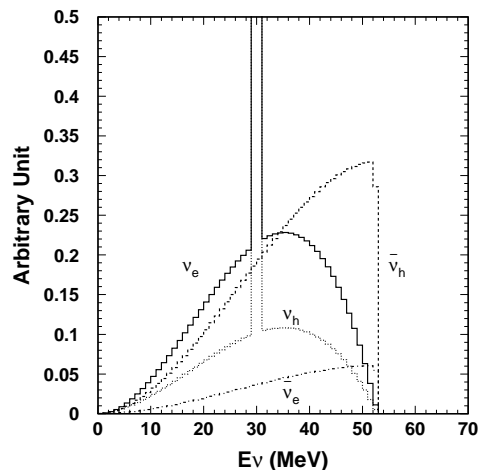


Fig. 1. Expected neutrino spectra at SK detector. Neutrino oscillation effect is taken into account.  $\mu, \tau$  components are grouped together as  $h$  since these two flavor neutrinos have the same cross section in electron scattering.

After going through neutrino oscillation, all neutrino species appear when they arrive at the Earth (Fig. 1), and such low energy neutrino events can be detected by a water Cherenkov detector.

## II. DETECTOR AND EXPECTED SIGNAL

We searched for monopole-induced neutrinos using Super-Kamiokande (SK) [10], a large water Cherenkov detector located at Kamioka mine in Japan. SK is a high-performance neutrino detector consisting of 11,146 20-inch PMTs and 50,000 tons of pure water. The fiducial volume of this search, which amounts to 22,500 tons, is defined to be more than 2 meters from the walls of the inner detector as there are gamma ray backgrounds near the wall. Monopole-induced neutrinos includes all six types of neutrinos, and electron scattering ( $\nu_x(\bar{\nu}_x) + e^- \rightarrow \nu_x(\bar{\nu}_x) + e^-$ ) in the fiducial volume is used for the monopole-induced neutrino search. Fig. 2 shows the recoil electron spectra in SK, where the values of the reference [11] are used as neutrino oscillation

parameters. Matter effects on oscillation in the Sun are also taken into account.

### III. DATA REDUCTION

In this analysis, 1496 days' data of SK-I taken from April 1996 to July 2001 is used. The backgrounds to the monopole-induced neutrino search are mainly atmospheric neutrinos and muon-induced spallation products. To minimize the contribution of the latter backgrounds, the lower energy threshold in this analysis is 18 MeV in total electron energy. The higher energy threshold is set to be 55 MeV, which is the end-point of the recoil electron spectrum (Fig. 2).

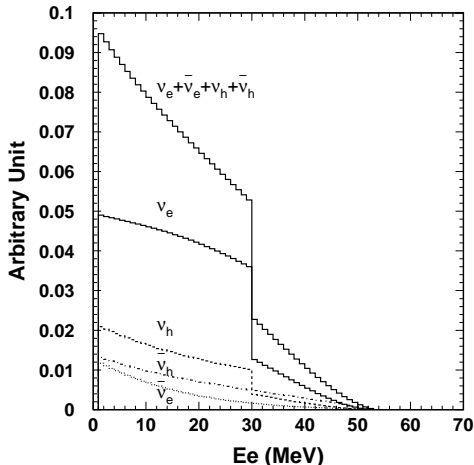


Fig. 2. Recoil electron spectrum in the SK described analytically without energy resolution included. How to read this figure is the same of Fig. 1

Besides setting the fiducial volume and energy criteria, some other background reductions are additionally applied to the data. After a “standard cuts” (total charge cut, outer detector trigger cut, flasher event cut, etc...), the data are subjected to a normal spallation cut. Cosmic ray muons can spall oxygen and induce unstable nuclei called spallation products ( $\mu + {}^{16}\text{O} \rightarrow \mu + \text{X}$ ). It is one of the most abundant backgrounds in  $< \sim 20$  MeV region, and as described above, the ability to remove the background determines the lower threshold of the monopole-induced neutrino search. The spallation background is reduced by a likelihood method that uses timing and track information of the muons preceding the candidate events. The same algorithm is used in the standard solar neutrino analysis of SK. In addition to the normal spallation cut, a tighter criterion is then applied in order to enhance the rejection efficiency of spallation background. The spallation products with the shortest half lives, such as  ${}^{11}\text{Li}$  and  ${}^{12}\text{N}$ , tend to create spallation events with the highest energies. So, we remove events which occur within 0.15 sec from cosmic ray muons.

Next, a Cherenkov angle cut is applied to the remaining data set. The remaining muons are removed by

this cut. The source of muons is from the interaction of atmospheric muon neutrinos. Electrons with  $E > 18$  MeV have a Cherenkov angle of  $\theta_C \sim 42^\circ$ . Muons that still remain in the monopole-induced neutrino search have  $p_\mu$  less than  $\sim 350\text{MeV}$ , which corresponds to  $\theta_C \sim 38^\circ$ ; thus, the events with  $\theta_C < 38^\circ$  were removed from the data. The Cherenkov angle cut is also used to remove events with  $\theta_C > 50$  degrees, which eliminates events without a clear Cherenkov ring pattern, such as multiple  $\gamma$  rays emitted by a nuclear de-excitation.

Some events originating from outside of the fiducial volume have the possibility of being reconstructed within the fiducial volume of SK.  $\gamma$ -rays from the materials of the detector structure and surrounding rock are the source of these backgrounds. To remove such events, the reconstructed direction is projected backwards from the vertex position until it reaches the inner detector wall, and events with this distance between the vertex and the wall greater than 450 cm are removed from the data.

Finally, charged current interactions of atmospheric  $\nu_\mu$  produce muons and decay electrons. Some low energy muons ( $\sim 160$  MeV) or decay electrons survive in this analysis but are tagged by preceding muons. Some fraction of those muons which passed the Cherenkov angle cut can be identified by the following decay electron. In order to remove those backgrounds we eliminate the events which have time-correlated events before or after the candidate events. However, the decay electrons whose mother muons are invisible (below Cherenkov threshold), Michel electrons, cannot be dropped by this cut; how to handle these events is described later.

### IV. ANALYSIS AND RESULTS

The energy spectrum after each selection criterion is shown in Fig. 3. After all cuts are applied, 163 monopole-induced neutrino candidates remain in the energy range from 18 MeV to 55 MeV. Most these candidates are due to three kinds of irreducible backgrounds.

The first background is spallation events from cosmic ray muons which still remain past the two spallation cuts described above.

The other two backgrounds are  $\nu_e$  and  $\nu_\mu$  components of atmospheric neutrinos. The “ $\nu_e$  component” means atmospheric  $\nu_e$  and  $\bar{\nu}_e$ , while the “ $\nu_\mu$  component” is atmospheric  $\nu_\mu$  and  $\bar{\nu}_\mu$  which produce muons below Cherenkov threshold whose decay electrons are then observed in the detector (invisible muon). The spectrum of these “invisible muons” is a Michel spectrum.

To subtract these backgrounds, angular distribution with respect to the direction of the Sun was used. As shown in Fig. 4, the data are divided into 20 angle bins and the following  $\chi^2$  function is minimized with respect to  $\alpha$  for each  $\beta$ .

$$\chi^2(\alpha, \beta) \equiv \sum_{i=1}^{20} \frac{\{N_{\text{real}}(i) - \alpha N_{\text{flat}}(i) - \beta N_{\text{MC}}(i)\}^2}{\sigma_i^2} \quad (4)$$

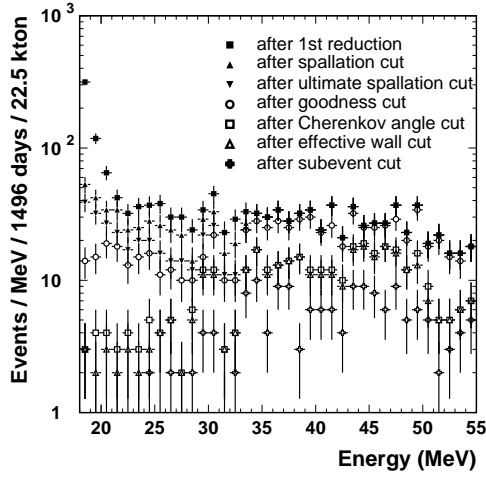


Fig. 3. Spectrum of data at each reduction step

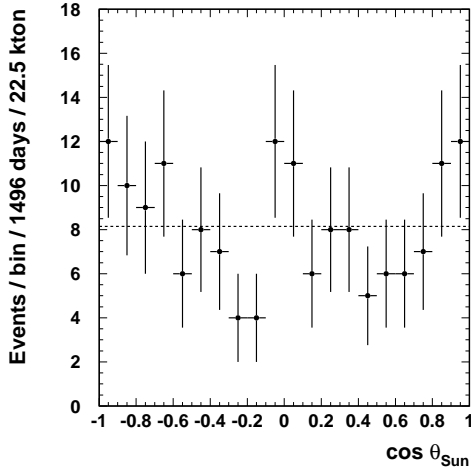
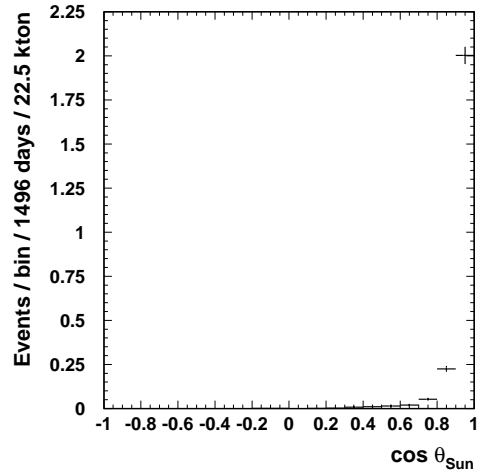


Fig. 4. Angular distribution with respect to the direction of the Sun of the remaining 163 events. The horizontal axis shows the cosine of the angle between the solar direction and the reconstructed direction of an event. The average value is shown by the horizontal dotted line.

Here, we use  $N_{\text{real}}(i)$  as the number of observed events for the  $i$ th bin. Because the background shape is thought to be almost symmetric with respect to the direction of the Sun, the number of the background events in the same exposure time is set to 0.05 for any  $i$ th bin and expressed as  $N_{\text{flat}}(i)$ .  $N_{\text{MC}}(i)$  means the number of expected signal events for  $i$ th bin (Fig. 5) calculated by Monte Carlo simulation.  $\sigma_i^2$  should be  $\sigma_{\text{stat},i}^2 + \sigma_{\text{sys},i}^2$ , but this time we haven't included the systematic error yet, and therefore set its value to zero for every  $i$ . Finally, we obtained  $\beta = 11.5$  events as upper limit at 90 % C.L.

These 11.5 events correspond to the following limit on the total monopole-induced neutrino flux,

$$I_0 < 3.9 \times 10^2 (B_{\pi^+}/0.5) \text{ cm}^{-2} \text{ s}^{-1} \text{ (90\%C.L.)} \quad (5)$$


 Fig. 5. Expected angular distribution of the signal, where the total monopole-induced flux is set equal to 90% C.L. upper limit obtained from the analysis in this paper,  $3.9 \times 10^2 \text{ cm}^{-2} \text{ s}^{-1}$ .

where  $B_{\pi^+}$  ( $\sim 0.5$  for several GUT models) is the branching ratio of proton decay into  $\pi^+$  + anything. The rate of monopole-catalyzed proton decay in the Sun is given by,

$$f_p = \int n_M \sigma v_{\text{rel}} \rho_H N_A d^3x \text{ decay/s} \quad (6)$$

where  $n_M$  is the monopole number density,  $\sigma$  the catalysis cross section,  $V_{\text{rel}} = \beta_{\text{rel}} c$  the relative velocity between the monopole and the hydrogen,  $\rho_H$  the hydrogen weight density, and  $N_A$  Avogadro's number ( $6.0 \times 10^{23}$ ). Helium gives a negligible contribution [12]. Assuming the monopoles are accumulated at the center of the Sun ( $\rho_H = 55 \text{ g/cm}^3$ ,  $\beta_{\text{rel}} = 1.7 \times 10^{-3}$ ), one obtains,  $f_p < 9.0 \times 10^{29} (0.5/B_{\pi^+}) \text{ s}^{-1}$  (90% C.L.). The rate  $f_p$  is further expressed as  $f_p = 4\pi d^2 I_0 / 3/R_{\nu_e}$ , where  $d$  is the distance between the Sun and the Earth ( $1.5 \times 10^8 \text{ km}$ ),  $R_{\nu_e} = B_{\pi^+} (1 - A_{\pi^+})$  the number of  $\nu_e$  produced in a proton decay.  $A_{\pi^+}$  (0.2) is the absorption probability of  $\pi^+$  at the center of the Sun [7]. From the above arguments and the limits on  $I_0$ ,

$$N_M \left( \frac{\sigma_0}{1 \text{ mb}} \right) \left( \frac{B_{\pi^+}}{0.5} \right) < 1.6 \times 10^{18} \text{ (90\%C.L.)} \quad (7)$$

The monopole flux is calculated from the following equation, assuming monopole-antimonopole annihilation is negligible,

$$N_M = \pi R_{\odot}^2 \left( 1 + \left( \frac{\beta_{\text{esc}}}{\beta_M} \right)^2 \right) 4\pi F_M t_{\odot} \quad (8)$$

where  $\beta_{\text{esc}}$  is the escape velocity ( $2 \times 10^{-3}$ ),  $t_{\odot}$  the time elapsed after the birth of the Sun ( $4.5 \times 10^9 \text{ yr}$ ). This leads to ( $\beta_M < 10^{-3}$ ),

$$F_M \left( \frac{\sigma_0}{1 \text{ mb}} \right) \left( \frac{B_{\pi^+}}{0.5} \right) < 1.5 \times 10^{-23} \left( \frac{\beta_M}{10^{-3}} \right)^2 \text{ cm}^{-2} \text{ s}^{-1} \text{ sr}^{-1} \text{ (90\%C.L.)} \quad (9)$$

This limit is not immediately applicable to monopoles heavier than  $10^{17}$  GeV, since the probability for the Sun to trap monopoles decreases as their masses become heavier.

Fig. 6 shows limits on the monopole flux for various masses. This is one order of magnitude more stringent a limit than the previous result, which was obtained by the Kamiokande experiment [13], [14].

The present limit may be compared with the one obtained from the X-ray excess of old neutron stars,

$$F_M \left( \frac{\sigma_0}{1\text{mb}} \right) \beta_{\text{rel}} < 3r \times 10^{-23} \text{ cm}^{-2} \text{ s}^{-1} \text{ sr}^{-1} \quad (10)$$

where  $\beta_M$  is  $10^{-3}$ ,  $r$  the ratio of the total (neutrino + photon) intensity to the photon intensity of old neutron stars, and takes a value [15] between 1 and  $10^4$ .  $\beta_{\text{rel}}$  in old neutron stars is of order of  $0.1 \sim 0.3$ . It is noted that the present limit depends on less ambiguous assumptions than that derived from old neutrons stars.

## V. CONCLUSION

In conclusion, this experiment has not found any evidence for monopole-catalyzed proton decay. The limits for the monopole flux are shown in Fig. 6.

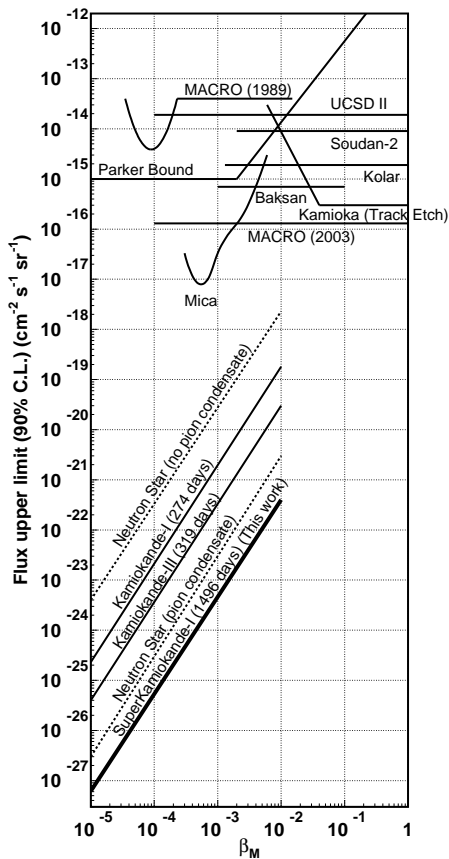


Fig. 6. 90% C.L. upper limits on the monopole flux as a function of monopole velocity,  $\beta_M$ . Catalysis cross section,  $\sigma_0$ , is assumed.

## REFERENCES

- [1] T.W.B.Kibble, J. Phys. **A9** (1976) 1387.
- [2] A.H.Guth, Phys. Rev. **D23** (1981) 347.
- [3] K.Sato, Phys. Lett. B **99** (1981) 66.
- [4] E.N.Parker, Astrophys. J. **160** (1970) 383; M.S.Turner et al., Phys. Rev. **D26** (1982) 1296.
- [5] G.Lazarides, C.Panagiotakopoulos, and Q.Shafi, Phys. Rev. Lett. **58** (1987) 1707.
- [6] S.Dar, Q.Shafi, and A.Sil, Phys. Rev. **D74** (2006) 035013.
- [7] J.Arafune and M.Fukugita, Phys. Lett. B **133** (1983) 380.
- [8] V.A.Rubakov, Pis'ma Zh. Eksp. Theor. Fiz. **33** (1981) 658 [JETP Lett. **33** (1981) 644]; Nucl. Phys. **B203** (1982) 311; V.A.Rubakov and M.S.Serbryakov, Nucl. Phys. **B218** (1983) 240.
- [9] C.G.Callan, Phys. Rev. **D25** (1982) 2141; **D26** (1982) 2058.
- [10] S.Fukuda et al., Nucl. Instr. and Meth. A **501** (2003) 418.
- [11] M. Maltoni et al., arXiv:hep-ph/0405172.
- [12] J.Arafune and M.Fukugita, Phys. Rev. Lett. **50** (1983) 1901.
- [13] T.Kajita et al., JPSJ **54** (1985) 4065.
- [14] A.Sakai, master thesis (1993).
- [15] E.W.Kolb and M.S.Turner, Astrophys.J. **286** (1984) 624.